Viscosity contrast effects on fingering formation in rotating Hele-Shaw flows

José A. Miranda*
Laboratório de Física Teórica e Computacional, Departamento de Física, Universidade Federal de Pernambuco, Recife, Pernambuco 50670-901, Brazil

Enrique Alvarez-Lacalle†
Department of Physics of Complex Systems, Weizmann Institute of Science, Rehovot, Israel
(Received 18 April 2005; published 26 August 2005)

The different finger morphologies that arise at the interface separating two immiscible fluids in a rotating Hele-Shaw cell are studied numerically. The whole range of viscosity contrast is analyzed and a variety of fingering patterns systematically introduced, including the case in which the inner fluid is less viscous than the outer one. Our numerical results demonstrate that both the magnitude and the sign of the viscosity contrast strongly affect the shape of the emerging fingers, and also their length distribution. We have also found that the occurrence and location of pinch-off singularities are remarkably modified when the inner fluid is less viscous: instead of generating an isolated detaching drop, a full finger is disconnected from the interface. Finally, we have verified that the finger competition phenomena revealed by our simulations are correctly predicted by a weakly nonlinear analysis of the pattern development, showing that such important finger competition dynamics is already set at relatively early stages of interfacial evolution.

DOI: 10.1103/PhysRevE.72.026306 PACS number(s): 47.54.+r, 47.20.Ma, 47.11.+j, 47.55.Dz

I. INTRODUCTION

During the last few years one particular variation of the classical viscous fingering problem [1] has attracted considerable attention of both theorists [2–16] and experimentalists [3,8,16–18]: it refers to the study of pattern formation in radial Hele-Shaw cells with rotation. In this "rotating" version of the problem, a Hele-Shaw cell of gap spacing b turns around an axis perpendicular to the plane of the flow with constant angular velocity Ω (Fig. 1). Inside the cell an initially circular droplet (radius R) of the more dense fluid 2 is surrounded by an outer fluid 1. The densities and viscosities of the fluids are denoted by ρ_j and η_j, respectively $(j=1,2)$, and between the fluids there exists a surface tension σ. The interfacial instability is driven by centrifugal forces leading to the formation of visually striking patterns. Generally speaking, these patterns present fingering structures in which a central drop of the more dense fluid throws out attached droplets, which themselves may form new droplets and fingers. At the same time, the fingers of the outer fluid advance toward the center of the cell. As a result a wealth of interesting phenomena related to finger competition dynamics, filament thinning, and interface pinch-off are revealed.

Pattern formation in rotating Hele-Shaw systems has been investigated during early, intermediate, and advanced stages of interfacial evolution. The stability of the evolving interface at early stages of pattern development has been studied analytically by linear stability analysis [2–5]. Other theoretical work examined key morphological aspects occuring at intermediate flow regimes through perturbative weakly nonlinear approaches [6,7]. Fully nonlinear, advanced stages have been investigated by numerical simulations [8–11,16] and experiments [3,8,16–18]. Finally, particular families of exact solutions have also been found [12–16].

By employing Hele-Shaw equations with standard boundary conditions to confined rotating flows, it is possible to show [6,7] that the most important morphological features of the emerging patterns can be properly described in terms of two dimensionless parameters: the viscosity contrast (or the dimensionless viscosity difference)

$$A = \frac{\eta_2 - \eta_1}{\eta_2 + \eta_1}, \tag{1}$$

and the effective surface tension coefficient

$$B = \frac{\sigma}{R^3\Omega^2(\rho_2 - \rho_1)}, \tag{2}$$

which measures the ratio of capillary to centrifugal forces [19]. Interestingly, the vast majority of theoretical [2–6,8–16] and experimental [3,8,16–18] studies focus exclusively on the case in which the inner fluid is more viscous, in such a way that the viscosity contrast is usually

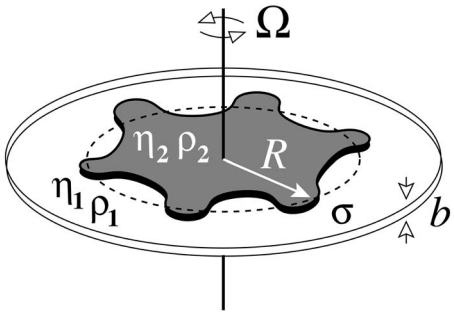

FIG. 1. Sketch of a rotating Hele-Shaw cell.

*Email address: jme@df.ufpe.br
†Email address: feenric@wisemail.weizmann.ac.il

viewed as a *positive* quantity. In contrast, the situation in which A is *negative* (inner fluid is less viscous but more dense) has been much less explored in the literature [7]. Fluid combinations leading to a negative viscosity contrast situation abound, and the patterns produced could possibly result in the rising of new and interesting structures at fully advanced stages. Nevertheless, preparing a circular initial condition is not straightforward and may represent a challenge for experimentalists, because the circular interface can be unstable when the inner fluid is initially introduced into the cell.

Very recently, Gadêlha and Miranda [7] have made important analytical predictions about the role of A for finger dynamics in rotating cells, taking into account all allowed values for the viscosity contrast, including negative ones. Considering the length variability as a measure of the finger competition, it has been predicted that competition among the fingering structures is dramatically modified as A varies: increasingly larger values of the magnitude of $A<0$ ($A>0$) lead to enhanced competition among outward (inward) fingers. It has been also predicted that competition is significantly suppressed when $A\to 0$. Regarding the role of B, it has been found that, besides setting the typical number of fingers formed at the onset of the instability, smaller values of B lead to more appreciable differences in finger competition behavior when induced by changes in A. Although the weakly nonlinear results of Ref. [7] are consistent with existing experimental and numerical investigations of the problem in both the high [3] and low [8] positive A limit, the validity of their suggestive findings to fully nonlinear stages and to all allowed values of $-1\leqslant A\leqslant +1$ is still unproved. In particular, the morphological details of the different patterns generated when A is varied, and their nonlinear dynamics still need to be addressed.

In this work, we perform intensive numerical simulations of the rotating Hele-Shaw problem, focusing on the impact of the viscosity contrast on the morphology, pinch-off, and dynamical behavior of the fluid-fluid interface. We examine the variations in the pattern morphology due to changes in A in both magnitude and sign, and identify the main differences among them. We also check the interesting predictions of Ref. [7] regarding finger competition dynamics.

II. NUMERICAL APPROACH AND GOVERNING EQUATIONS

Our numerical study is based on the vortex sheet representation for Hele-Shaw flow [20]. The fluid-fluid boundary is described by a simple closed curve parametrized by arclength s, where the evolution of the interface position $[d\mathbf{r}(s,t)/dt]\cdot\hat{\mathbf{n}}=\mathbf{w}(s,t)\cdot\hat{\mathbf{n}}$ is obtained by using Darcy's law for the two-dimensional velocity $\mathbf{v}$ in the bulk of the flow, and the standard boundary conditions at the interface [2,3]: (i) the pressure jump at the interface $p_2-p_1=\sigma\kappa$, where κ denotes the interface curvature and p_j represents the hydrodynamic pressure; and (ii) the kinematic boundary condition $\hat{\mathbf{n}}\cdot\mathbf{v}_1=\hat{\mathbf{n}}\cdot\mathbf{v}_2$, which refers to the continuity of the normal velocity across the interface ($\hat{\mathbf{n}}$ is the unit normal to the interface).

The moving boundary problem can then be written uniquely in terms of the shape of the interface. The self-consistent equation for the velocity $\mathbf{w}(s,t)$ of the interface due to a vortex sheet is given by the Birkhoff integral formula [20,21]

$$\mathbf{w}(s,t)=\frac{1}{2\pi}\mathrm{P}\int ds'\frac{\hat{\mathbf{z}}\times[\mathbf{r}(s,t)-\mathbf{r}(s',t)]}{|\mathbf{r}(s,t)-\mathbf{r}(s',t)|^2}\gamma(s',t), \quad (3)$$

where P means a principal-value integral and $\hat{\mathbf{z}}$ is the unit vector along the direction perpendicular to the cell. The function $\gamma(s,t)$ is the vorticity generated by the discontinuity of the tangential velocity at the interface. The velocity introduced in Eq. (3) is an average velocity of the interface defined as $\mathbf{w}=(\mathbf{v}_1+\mathbf{v}_2)/2$, where $\mathbf{v}_1$ and $\mathbf{v}_2$ are the two limiting values (from both sides of the interface) of the solenoidal part of the velocity at a given point. By rescaling lengths by R and velocities by $U=[b^2R(\rho_2-\rho_1)\Omega^2]/[12(\eta_1+\eta_2)]$ it can be shown that the vortex sheet strength (or vorticity) can be conveniently written in a dimensionless form, in terms of the parameters A and B, as [6,20]

$$\gamma=2[A\mathbf{w}\cdot\hat{\mathbf{s}}-r\hat{\mathbf{r}}\cdot\hat{\mathbf{s}}+B\partial_s\kappa], \quad (4)$$

where $\hat{\mathbf{s}}=\partial_s\mathbf{r}$ is the unit counterclockwise tangent vector along the interface.

To obtain the evolution of the interface, Eq. (4) has to be solved with $\mathbf{w}$ given by Eq. (3), yielding an integro-differential equation for the vorticity. Once γ is known, Eq. (3) is used again to obtain $\mathbf{w}$, and then its normal component is used to update the position of the interface. To solve these equations numerically, we adapt a code originally developed by Pauné, Siegel, and Casademunt [22,23] to study flow in both circular and rectangular Hele-Shaw cells that removes the stiffness produced by surface tension. Further details on the implementation and quantitative validation of this numerical scheme can be found in Refs. [6,24–27].

III. RESULTS AND DISCUSSION

Numerical simulations showing the effects of A and B on the evolution of the patterns are shown in Fig. 2. The rows in Fig. 2 are arranged according to B: top row (a)–(d) for $B=5.0\times10^{-4}$; middle row (e)–(h) for $B=10^{-3}$; and bottom row (i)–(l) for $B=10^{-2}$. The columns are arranged according to the values of viscosity contrast: $A=-1$ (a), (e), (i), $A=-0.5$ (b), (f), (j), $A=0$ (c), (g), (k), and $A=+1$ (d), (h), (l). For clarity, only the final pattern and the boundary of the initially circular droplet are shown. For the results presented in this work, all numerical experiments begin with the same initial state of a circle centered on the axis of rotation with a small amount of random noise distributed in the first 50 azimuthal modes. The numerical simulation are stopped when the pinch-off process renders the simulation inaccurate.

We begin our analysis by describing general morphological features of the patterns and the main distinctions among them when the parameters A and B are changed. First, we observe that the resulting patterns shown in Figs. 2(a), 2(e), and 2(i) for negative viscosity contrast $A=-1$ present a series of peculiar petal-like structures. The outward fingers are con-

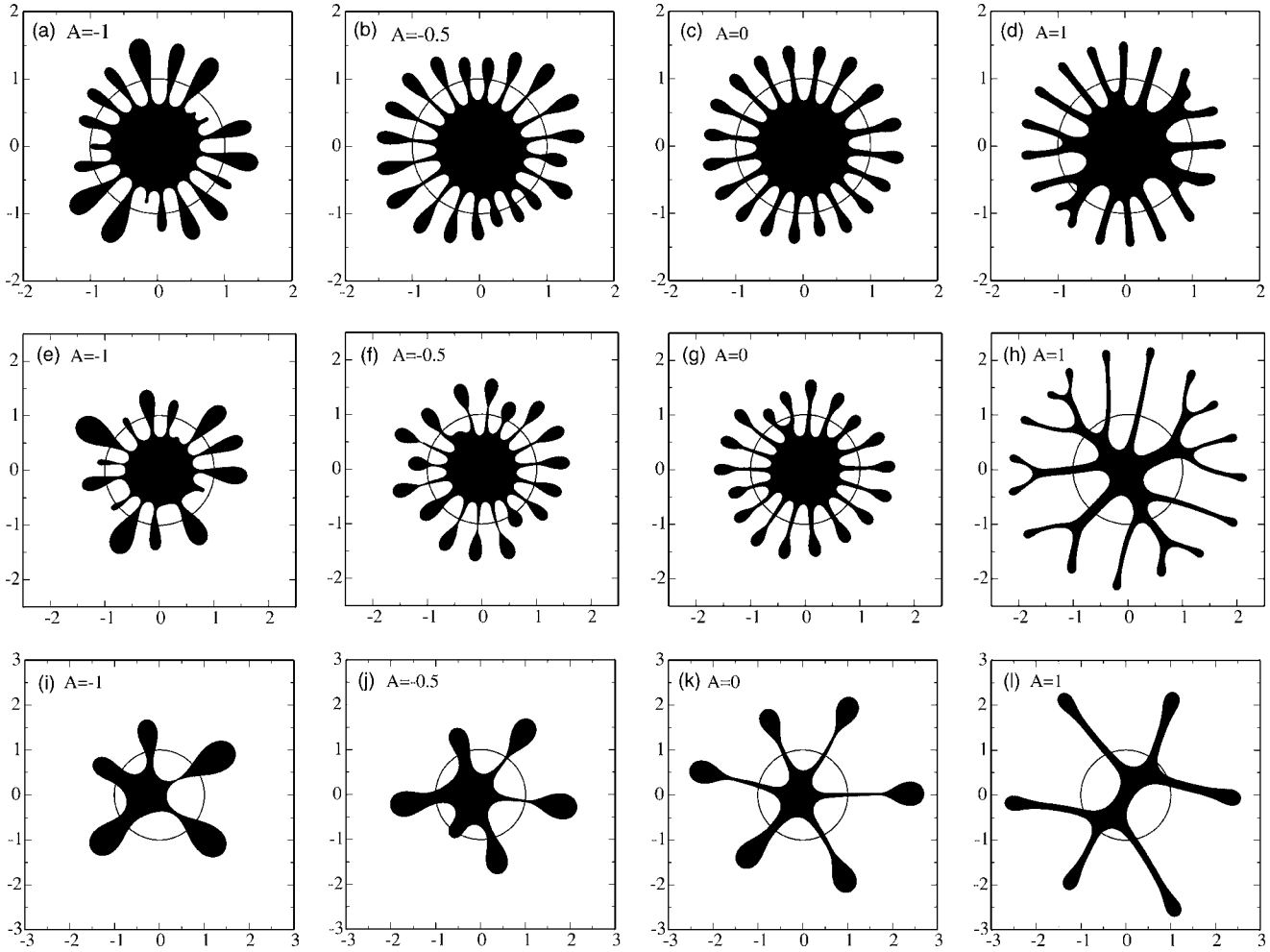

FIG. 2. Numerical experiments showing the development of typical fingering patterns in a rotating Hele-Shaw cell for four values of viscosity contrast $A=-1$, -0.5, 0, and 1 as labeled, and three values of the surface tension parameter $B=5.0\times10^{-4}$ (top row), 10^{-3} (middle row), and 10^{-2} (bottom row). Only the border of the initial droplet (circular line) and the final pattern (in black) are shown.

siderably wider at the tips, and tend to pinch off at the bottom, in a region near the rotation axis. It is clear that the basic difference among these patterns is essentially the number of fingers, which is larger for smaller values of B.

For intermediate negative viscosity contrast $A=-0.5$ Figs. 2(b), 2(f), and 2(j), the position of pinch-off moves from a region closer to the rotation axis toward the tip of the finger. As we can see, increasing viscosity contrast can lead to a pinch-off process at different points along the finger. The fingers also became less wide and in general present a more noticeable resemblance in their shapes. At this point, it is important to recall that in all the plots depicted in Fig. 2 the initial conditions have not been prepared in any way. It is the dynamic influence of viscosity contrast which produces different length distribution and competition processes even for negative viscosity contrasts. We also point out that, in contrast to the case in which $A>0$, our specific numerical predictions for negative viscosity contrasts have not yet been subjected to experimental check.

Now we examine the case of viscosity-matched fluids, and try to identify the characteristic interfacial behavior in the ideal limit $A\rightarrow0$ [Figs. 2(c), 2(g), and 2(k)]. It is noticed that for $A=0$ the outward fingers tend to stretch radially, resulting in a fairly regular array of fingering structures presenting bulbous ends. The development of thin filaments connected to relatively large droplets which tend to pinch at the end of the fingers is very clearly depicted in Figs. 2(g) and 2(k). Note that in contrast to the case shown in Figs. 2(a), 2(e), and 2(i) for $A=-1$ and Figs. 2(b), 2(f), and 2(j) for $A=-0.5$, droplet pinch-off now tends to occur far from the rotation axis, near the tip of the elongated outward fingers. This is in agreement with recent experiments performed in rotating Hele-Shaw cells in the limit of very low $A>0$ and σ [8]. In fact, the general features characterizing tendency toward pinch-off for $A=0$ and $A=-0.5,-1$ are quite different: while the fingers have to stretch, and then pinch near the tips when $A=0$, for negative A the fingers inflate as a whole and pinch-off occurs near their bases, regardless of the fact that the interface has not been stretched outward. So the mechanisms (with and without stretching) and location of pinch-off seem to depend significantly on the value and sign of A.

We proceed by discussing the most studied case $A=+1$. In Figs. 2(d), 2(h), and 2(l) we observe branched, backbone structures which are characterized by the fact that, for a given B, the width of the fingers remain approximately constant along their lengths. By comparing the patterns for vari-

ous A in Fig. 2, it is evident that the characteristic width of the fingers is also quite sensitive to changes in A. In contrast to the case $A=0$, when $A=+1$ it is clear that the inner fluid does not accumulate at the ends of the fingers, so that we see no tendency toward "neck" pinch-off. It is also worth noting the absence of pinching at the base of the fingers, as opposed to what is verified in the case $A=-1$. On this basis, it seems that pinch-off events are not systematically favored when $A=+1$.

Now we turn our attention to the finger competition dynamics. Length variability of outward fingers is quite evident in Figs. 2(a), 2(e), and 2(i) ($A=-1$) characterizing a strong competition among them. Conversely, the inward moving fingers of the outer fluid do not compete as much. This last feature is more clearly illustrated in Figs. 2(a) and 2(e), (for smaller values of B), where the tips of the inward penetrating fingers delineate an approximately circular internal region around the center of the pattern. It is also apparent that the patterns generated for intermediate values of negative A($A=-0.5$) present less dramatic competition. On the other hand, the most noteworthy fact in Figs. 2(c), 2(g), and 2(k), for the zero viscosity case, is that there is basically no competition, in the sense that the average lengths of inward and outward fingers do not vary much. The fact that finger competition is suppressed for low viscosity contrast is a very well known fact for Hele-Shaw flow in rectangular geometry [20,28–31]. But for the rotating case, we specifically show that the situation $A=0$ establishes a sort of dividing point between two different types of competition: inward finger and outward finger competition. By inspecting Figs. 2(d), 2(h), and 2(l) ($A=1$) one can easily see that finger variability is much more intense among inward fingers which penetrate the inner fluid pretty strongly, while, as indicated before, for negative viscosity contrast the outward fingers have a much more variable length. This is validated by noting that when $A=1$ the shape of the internal part of fluid 2 is not circularly symmetric, as opposed to the more rounded internal parts obtained for $A=0$ and $A=-0.5,-1$. On the other hand, the typical sizes of the structures moving outward do not change significantly in Figs. 2(d), 2(h), and 2(l).

To illustrate these finger competition features in a more quantitative fashion, in Fig. 3 we take the same physical parameters used in Figs. 2(a), 2(c), and 2(d) for $B=5.0\times10^{-4}$ and plot the dimensionless radial coordinate (r/R) of the finger tips for each finger (n) (n is an integer, and labels the fingers) for $A=$(a)-1, (b) 0, and (c) 1. The filled (empty) circles locate the radial positions of the outward (inward) fingers. The finger competition features we have discussed above, by visually inspecting the patterns shown in Fig. 2, are strikingly confirmed by Fig. 3: $A=-1$ (1) leads to enhanced competition among outward (inward) fingers, and finger competition is considerably suppressed when $A=0$. As a matter of fact, one could say there is competition always in the direction of less viscous fingering penetrating into more viscous, regardless of whether they are going inward or outward. This indicates that the competition among the emerging fingering structures is primarily determined by a viscosity-driven mechanism in the nonlocal and nonlinear terms of the dynamics, as is the case in the purely viscosity-driven Saffman-Taylor instability [1].

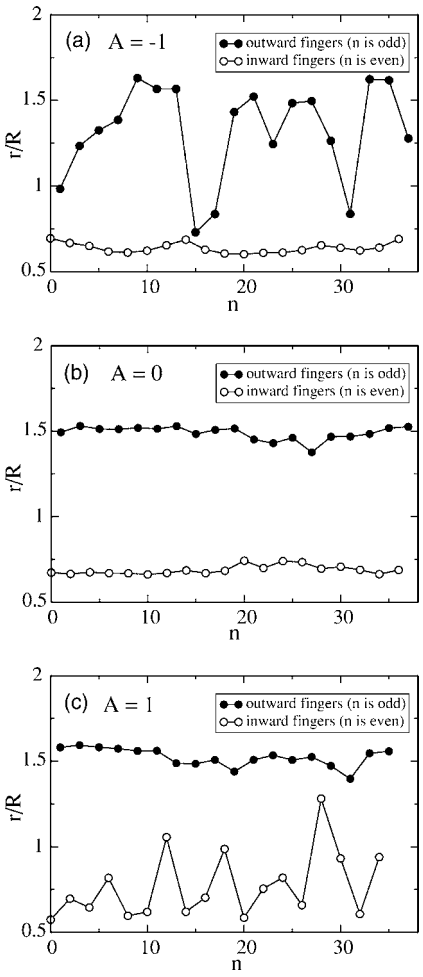

FIG. 3. Dimensioness radial coordinate r/R of the finger tip for each finger n (n is an integer) at the interface, when $B=5.0\times10^{-4}$ and $A=$(a)-1, (b) 0, and (c) 1. These data are taken from the patterns obtained in Figs. 2(a), 2(c), and 2(d).

IV. CONCLUDING REMARKS

Our numerical results substantiate the analytical predictions of Ref. [7], providing a convincing evidence of the usefulness of their weakly nonlinear approach. The very good agreement between our numerical results and the analytical findings of Ref. [7] indicates that finger competition is already set at relatively early stages of interfacial evolution. Moreover, our simulations reinforce the fact that the viscosity contrast A plays a crucial role in determining the pattern morphology, in the sense that changes in its magnitude and sign result in fingering patterns presenting very different typical lengths and widths. In particular, we have shown that the patterns generated for negative viscosity contrast are very distinct from those obtained when $A\geqslant0$. Our numerical findings also seem to indicate that A has a key role in the dynamics of interfacial singularities (pinch-off events) not only as to whether this pinch-off would appear at finite or at infinite time [16], but also in the similarly basic question of what the eventual location of the pinching would be. Our results show that the pinch-off position moves away from the rotation axis for increasingly larger values of A. Given the

fact that the analytical approach to this process is based on the lubrication approximation [16], and that this fails when $A=-1$, addressing this issue becomes an interesting open theoretical question.

A possible extension of the current work is the investigation of the influence of magnetic forces on the morphological properties of interfaces in rotating Hele-Shaw cells. This can be done by assuming that the inner, more dense fluid is a ferrofluid (or magnetic fluid) [32], and a magnetic field is applied. Depending on the symmetry properties of the applied magnetic field (for instance, azimuthal [4,10] or perpendicular [33]) it can either stabilize or destabilize the interface. Among other things, an external magnetic field could be used to suppress the occurrence of interfacial singularities [34]. It would be of interest to study how the magnetic field couples to the parameters A and B, possibly leading to nontrivial nonlinear behaviors and even more complex interfacial morphologies. Another interesting variation of the current immiscible situation would be to examine how finger competition dynamics and pinch-off events would be modified if the confined rotating fluids were miscible [9,11]. Miscible fluids present negligible interfacial tension, but the consideration of unusual stresses (for instance, Korteweg stresses [11,35,36]) may lead to dynamic surface-tension-like effects, a fact that may provide useful ways of further testing our current immiscible results.

ACKNOWLEDGMENTS

J. A. M. thanks CNPq (Brazilian Research Council) for financial support of this research through the CNPq/FAPESQ Pronex program. E.A.-L. acknowledges financial support from the PHYNECS European Network for the mobility and training of researchers. We are greatly indebted to E. Pauné and J. Casademunt for important discussions and useful suggestions. It is a pleasure to thank E. Pauné for the use of his numerical code as a starting point of our simulations.

[1] P. G. Saffman and G. I. Taylor, Proc. R. Soc. London, Ser. A **245**, 312 (1958).
[2] L. W. Schwartz, Phys. Fluids A **1**, 167 (1989).
[3] Ll. Carrillo, F. X. Magdaleno, J. Casademunt, and J. Ortín, Phys. Rev. E **54**, 6260 (1996).
[4] J. A. Miranda, Phys. Rev. E **62**, 2985 (2000).
[5] S. L. Waters and L. J. Cummings, Phys. Fluids **17**, 048101 (2005).
[6] E. Alvarez-Lacalle, E. Pauné, J. Casademunt, and J. Ortín, Phys. Rev. E **68**, 026308 (2003).
[7] H. Gadêlha and J. A. Miranda, Phys. Rev. E **70**, 066308 (2004).
[8] E. Alvarez-Lacalle, J. Ortín, and J. Casademunt, Phys. Fluids **16**, 908 (2004).
[9] C.-Y. Chen and S.-W. Wang, Fluid Dyn. Res. **30**, 315 (2002).
[10] D. P. Jackson and J. A. Miranda, Phys. Rev. E **67**, 017301 (2003).
[11] C.-Y. Chen and H.-J. Wu, Phys. Fluids **17**, 042101 (2005).
[12] V. M. Entov, P. I. Etingof, and D. Ya. Kleinbock, Eur. J. Appl. Math. **6**, 399 (1996).
[13] F. X. Magdaleno, A. Rocco, and J. Casademunt, Phys. Rev. E **62**, R5887 (2000).
[14] D. Crowdy, Q. Appl. Math. **60**, 11 (2002); SIAM J. Appl. Math. **62**, 945 (2001).
[15] E. Alvarez-Lacalle, J. Ortín, and J. Casademunt, Phys. Rev. Lett. **92**, 054501 (2004).
[16] R. Folch, E. Alvarez-Lacalle, J. Ortín, and J. Casademunt, e-print physics/0408092.
[17] Ll. Carrillo, J. Soriano, and J. Ortín, Phys. Fluids **11**, 778 (1999).
[18] Ll. Carrillo, J. Soriano, and J. Ortín, Phys. Fluids **12**, 1685 (2000).
[19] As far as notation is concerned, we point out that in Ref. [7] the definition of the viscosity contrast differs from the one given in Eq. (1) by a minus sign. On the other hand, we note that Ref. [6] uses an inverse effective surface tension parameter given by $S=1/B$.
[20] G. Tryggvason and H. Aref, J. Fluid Mech. **136**, 1 (1983).
[21] G. Birkhoff, Los Alamos Scientific Laboratory Technical Report No. LA-1862, 1954 (unpublished).
[22] E. Pauné, M. Siegel, and J. Casademunt, Phys. Rev. E **66**, 046205 (2002).
[23] E. Pauné, Ph.D. thesis, Universitat de Barcelona, 2002 (unpublished).
[24] H. D. Ceniceros, T. Y. Hou, and H. Si, Phys. Fluids **11**, 2471 (1999).
[25] H. D. Ceniceros and T. Y. Hou, J. Fluid Mech. **409**, 251 (2000).
[26] T. Hou, J. Lowengrub, and M. Shelley, J. Comput. Phys. **114**, 312 (1994).
[27] M. Siegel, S. Tanveer, and W. S. Dai, J. Fluid Mech. **323**, 201 (1996).
[28] G. Tryggvason and H. Aref, J. Fluid Mech. **154**, 287 (1985).
[29] J. Casademunt and D. Jasnow, Phys. Rev. Lett. **67**, 3677 (1991).
[30] J. V. Maher, Phys. Rev. Lett. **54**, 1498 (1985).
[31] M. W. DiFrancesco and J. V. Maher, Phys. Rev. A **39**, 4709 (1989); **40**, 295 (1989).
[32] R. E. Rosensweig, *Ferrohydrodynamics* (Cambridge University Press, Cambridge, U.K., 1985), and references therein.
[33] D. P. Jackson, R. E. Goldstein, and A. O. Cebers, Phys. Rev. E **50**, 298 (1994).
[34] J. A. Miranda and R. M. Oliveira, Phys. Rev. E **69**, 066312 (2004).
[35] D. Korteweg, Arch. Neerl. Sci. Ex. Nat. Ser. II **6**, 1 (1901).
[36] H. Hu and D. Joseph, ZAMP **43**, 626 (1992).